Supplementary Information

for

Unveiling the impact of oxidation-driven endogenous protein interactions on the dynamics of amyloid-β aggregation and toxicity

Zhi Du,[a,†] Eunju Nam,[a,†] Yuxi Lin,[b,†] Mannkyu Hong,[a,c] Tamás Molnár,[d] Ikufumi Kondo,[e] Koichiro Ishimori,[e,f] Mu-Hyun Baik,[a,c] Young-Ho Lee ,*[b,g,h,i] and Mi Hee Lim*[a]

[a]Department of Chemistry, Korea Advanced Institute of Science and Technology (KAIST), Daejeon 34141, Republic of Korea

[b]Research Center for Bioconvergence Analysis, Korea Basic Science Institute (KBSI), Ochang, Chungbuk 28119, Republic of Korea

[c]Center for Catalytic Hydrocarbon Functionalizations, Institute for Basic Science (IBS), Daejeon 34141, Republic of Korea

[d]Department of Biochemistry, Institute of Biology, Eötvös Loránd University, H-1117 Budapest, Hungary

[e]Graduate School of Chemical Sciences and Engineering, Hokkaido University, Kita 13, Nishi 8, Kita-ku, Sapporo 060-8628, Japan

[f]Chemistry Department, Faculty of Science, Hokkaido University, Kita 10, Nishi 8, Kita-ku, Sapporo 060-0810, Japan

[g]Bio-Analytical Science, University of Science and Technology (UST), Daejeon 34113, Republic of Korea

[h]Graduate School of Analytical Science and Technology, Chungnam National University, Daejeon 34134, Republic of Korea

[i]Research Headquarters, Korea Brain Research Institute (KBRI), Daegu 41068, Republic of Korea

[†]These authors contributed equally to this work.

*Corresponding Author: miheelim@kaist.ac.kr and mr0505@kbsi.re.kr

Table of Contents

Experimental Section

Experimental Section

Materials and Methods

All reagents were purchased from commercial suppliers and used as received unless otherwise stated. $A\beta_{42}$ (DAEFRHDSGYEVHHQKLVFFAEDVGSNKGAIIGLMVGGVVIA) was obtained from Peptide Institute, Inc. (Osaka, Japan) that was purified by high-performance liquid chromatography (HPLC) using YMC Pack ODS-A (YMC CO., LTD., Kyoto, Japan) and Agilent ZORBAX 300SBC18 columns (Agilent, Santa Clara, CA, USA), respectively. Cyt *c* from horse hearts was purchased from Sigma-Aldrich (St. Louis, MO, USA). Horse Cyt *c* was employed in gel/Western blot, CD spectroscopy, TEM, ESI–MS, ITC, and cell studies, and ^{15}N-labeled human Cyt *c* was used for 2D ^{1}H–^{15}N NMR experiments. It should be noted that Cyt *c* from mammals exhibits high identity in terms of the amino acid sequences and three-dimensional structures. HEPES [2-(4-(2-hydroxyethyl)piperazin-1-yl)ethanesulfonic acid] was obtained from SigmaAldrich. Double-distilled water (ddH_2O) used for all experiments was obtained from a Milli-Q Direct 16 system (Merck KGaA, Darmstadt, Germany). Trace metal contamination was removed from the solutions used for $A\beta_{42}$ experiments by treating Chelex (Sigma-Aldrich) overnight. The concentrations of proteins were determined by a Shimadzu 1900i UV-visible (UV-Vis) spectrophotometer (Shimadzu, Kyoto, Japan). Experiments by ESI–MS were performed by an Agilent 6530 Accurate Mass Quadrupole Time-of-Flight (Q-TOF) mass spectrometer with an ESI source (Agilent). 2D ^{1}H-^{15}N NMR measurements were conducted by a Bruker Avance II 800 NMR spectrometer [Bruker BioSpin, Rheinstetten, Germany; Korea Basic Science Institute (KBSI), Ochang, Republic of Korea] equipped with a cryogenic probe. ITC was performed by a VP-ITC instrument equipped with a motor-driven syringe (Malvern Panalytical, Malvern, UK). The membranes obtained by gel/Western blot were visualized by a ChemiDoc MP Imaging System (Bio-Rad, Hercules, CA, USA). The changes of the secondary structure of proteins were analyzed by a JASCO-815 150-L CD spectropolarimeter [Jasco Inc., Tokyo, Japan; KAIST Analysis Center for Research Advancement (KARA), Daejeon, Republic of Korea]. Morphological changes of protein aggregates were monitored by a Tecnai-G2 Spirit Twin instrument (FEI Company, Eindhoven, Netherlands). The R_H value of Cyt *c* was determined by a DynaPro PlateReader-II instrument (Wyatt Technology, CA, USA). MTT [3-(4,5-dimethylthiazol-2-yl)-2,5-diphenyltetrazolium bromide] was purchased from Sigma-Aldrich. Absorbance values for the MTT assay were determined by a SpectraMax M5e microplate reader (Molecular Devices, San Jose, CA, USA).

Expression and Purification of ^{15}N-Labeled Recombinant $A\beta_{42}$. ^{15}N-labeled $A\beta_{42}$ was

expressed recombinantly in *E. coli* and purified according to the previously reported methods with some modifications.[1] Briefly, the DNA sequence coding human $A\beta_{42}$ was artificially constructed using codons preferred by *E. coli* with an extra Met residue at the *N*-terminus of the peptide. The DNA construct was inserted into pAED4 vector[2] and the protein expression was carried out in *E. coli* BL21 (DE3) pLysS strain (Novagen, Inc., Madison, WI, USA). Transformed cells were grown in LB media containing ampicillin and chloramphenicol until the cultures reach 3.5 McFarland turbidity. Cells were then harvested, transferred into M9 minimal media containing ^{15}N-labelled ammonium chloride (1 g/L), and induced with IPTG (1 mM) for 4 h. The peptide accumulated in the form of inclusion bodies in the bacterial cells. The purified inclusion bodies were solubilized in NaOH (20 mM, aq) and the peptide was further purified by repeated cycles of amyloid growth at low pH and monomerization in hexafluoroisopropanol (HFIP) combined with centrifugation steps. The monomerized and lyophilized peptides were dissolved in NaOH (20 mM, aq) on ice and then purified further on a Source 15 RPC (Cytiva, Marlborough, MA) HPLC column. The preparation is ended with another HFIP monomerization step.

Preparation of $A\beta_{42}$ and Cyt *c*. $A\beta_{42}$ was dissolved in ammonium hydroxide (NH_4OH; 1% w/w, aq) and the resulting solution was aliquoted, lyophilized overnight, and stored at –80 °C. A stock solution of $A\beta_{42}$ was then prepared by dissolving the lyophilized peptide with NH_4OH (1% w/w, aq; 10 μL) and diluting with ddH_2O, as previously reported.[3] The concentration of $A\beta_{42}$ was determined by measuring the absorbance at 280 nm (ε_{280} = 1,490 $M^{-1}cm^{-1}$).[4] A stock solution of Cyt *c* (500 μM) was prepared by dissolving the protein in ddH_2O and stored at –20 °C. The concentration of Cyt *c* was determined by measuring the absorbance at 410 nm (ε_{410} = 106 $mM^{-1}cm^{-1}$).[5]

Gel/Western Blot. $A\beta_{42}$ was incubated with Zn(II), Cyt *c*, and H_2O_2 for 1, 2, 4, 8, and 12 h at 37 °C with constant agitation (250 rpm) in 150 mM HEPES, pH 7.4. The samples were prepared using Eppendorf tubes (Hamburg, Germany). The resultant samples were analyzed by gel/Western blot using an anti-Aβ antibody (6E10; Biolegend, San Diego, CA, USA) or an anti-Cyt *c* antibody (ab13575; Abcam, Cambridge, UK). Each sample (10 μL) was separated onto a tricine gel (10–20% w/v acrylamide; Invitrogen, Carlsbad, CA, USA). Following separation, the proteins were transferred onto nitrocellulose membranes and blocked with bovine serum albumin (BSA, 3% w/v; Sigma-Aldrich) in Tris-buffered saline (TBS) containing 0.1% v/v Tween-20 (Sigma-Aldrich) (TBS-T) for 3 h at room temperature. The membranes were incubated with anti-Cyt *c* (1:2,000) or 6E10 (1:2,000) in the solution of BSA (2% w/v in TBS-T) overnight at room

temperature. After washing with TBS-T three times (10 min), an alkaline phosphatase-conjugated goat anti-mouse secondary antibody (ab7069, 1:1,000; Abcam) in the solution of BSA (2% w/v in TBS-T) was added for 2 h at room temperature. 5-bromo-4-chloro-3'-indolyphosphate p-toluidine salt (BCIP)/nitro-blue tetrazolium chloride (NBT) liquid substrate system (Sigma-Aldrich) was used to visualize the images gained by gel/Western blot on an imaging system (Bio-Rad, Hercules, CA, USA).[6]

CD Spectroscopy. $A\beta_{42}$ was incubated with Zn(II), Cyt *c*, and H_2O_2 for 0, 1, 2, 4, 8, and 12 h in 20 mM sodium phosphate (NaPi), pH 7.4, 150 mM NaF. The samples were prepared using Eppendorf tubes. The CD spectra of the samples were collected in the range from 200 to 250 nm with a cell path length of 0.5 mm. The digital integration time, the bandwidth, and the scanning speed were 4 s, 2 nm, and 20 nm/min, respectively. The spectra of $A\beta_{42}$ with Cyt *c* were obtained by subtracting the features of Cyt *c* under the same conditions. Each spectrum was smoothed by Fourier transforms. The mean residue molar ellipticity [θ] (deg.cm^2.dmol^{-1}) was obtained by the equation (1):

$$[\theta] = \theta \times 100 / (C \times l \times n) \qquad (1)$$

where θ is the ellipticity in degrees; l is the optical path in cm; C is the concentration in mM; and n is the number of residues in the protein. The contents of secondary structures were analyzed from the CD spectra using the BeStSel program (http://bestsel.elte.hu/).[7]

TEM. Samples for TEM measurements were prepared based on previously published methods.[8] Glow-discharged grids (Formvar/Carbon 300-mesh, Electron Microscopy Sciences, Hatfield, PA, USA) were treated with the resultant samples for 2 min at room temperature. Excess sample was removed using a filter paper. Each grid was washed three times with ddH_2O and incubated with uranyl acetate (1% w/v ddH_2O; 5 μL) for 1 min. After removing excess uranyl acetate, the grids were dried overnight at room temperature. Images of each grid were taken at 300 kV with a magnification of 29,000x. For the TEM analysis, the location of samples on the grids was randomly selected for taking more than 15 images per each grid.

ESI–MS. $A\beta_{42}$ (100 μM) was incubated with Cyt *c* (100 μM), $ZnCl_2$ (100 μM) and H_2O_2 (1.6 mM) for 30 min at 37 °C in 20 mM ammonium acetate, pH 7.4. The samples were prepared using Eppendorf tubes (Hamburg, Germany). Before injection into the mass spectrometer, the resultant

samples were diluted by 10 fold with LC-grade H_2O. The capillary voltage, the drying gas flow, and the gas temperature were set to 5.8 kV, 12 L/min, and 300 ^oC, respectively. The ESI parameters and experimental conditions for tandem MS (ESI–MS^2) were the same as above. The collision-induced dissociation was conducted by applying the collision energy at 40 eV. The measurements were conducted in triplicate.

2D ^1H–^{15}N NMR Spectroscopy. The stock solution of ^{15}N-labeled Aβ_{42} were prepared as described previously with some modifications.[1] Briefly, a solution of ^{15}N-labeled Aβ_{42} monomer was prepared by dissolving the lyophilized peptide in the chilled NaOH solution (10 mM) to make a stock concentration of *ca*. 200 μM. The undissolved aggregates were removed by centrifugation at 40,000 rpm for 1 h. For 2D ^1H–^{15}N SOFAST-HMQC NMR measurements of ^{15}N-labeled Aβ_{42}, the stock solution was further diluted to be 40 μM of ^{15}N-labeled Aβ_{42} in 150 mM HEPES, pH 7.4 containing 10% v/v D_2O, and then treated with Cyt *c* (200 μM) and H_2O_2 (1.6 mM). Each SOFAST–HMQC spectrum was obtained from 128 t_1 experiments using 180 transients and 0.1 s recycle delay. For 2D ^1H–^{15}N HSQC NMR spectra of ^{15}N-labeled Cyt *c*, ^{15}N-labeled Cyt *c* was expressed and purified as previously described.[9] Then 20 μM of ^{15}N-labeled Cyt *c* was resolved in 20 mM HEPES, pH 7.4; 10% v/v D_2O and then treated with Aβ_{42} (100 μM) and H_2O_2 (160 μM). The NMR tube loaded with the sample was immediately placed into the NMR instrument. The NMR measurement time was *ca.* 1 h for ^{15}N-labeled Aβ_{42} and *ca.* 7 h for ^{15}N-labeled Cyt *c.* All spectra were obtained at 10 °C. Each HSQC spectrum was obtained from 256 t_1 experiments using 50 transients and 2 s recycle delay. All NMR spectra were obtained at 10 °C. Data were processed by NMRPipe and analyzed by Sparky.[10,11] The assignment of backbone resonance of ^{15}N-labeled Aβ_{42} and ^{15}N-labeled Cyt *c* was carried out based on the previous study.[12,13] Chemical shift perturbation (CSP; $\Delta\delta_{NH}$) was calculated by the equation (2):[14]

$$\Delta\delta_{NH} = \sqrt{\Delta\delta_H{}^2 + \left(\frac{\Delta\delta_N}{6.5}\right)^2} \qquad (2)$$

where $\Delta\delta_H$ and $\Delta\delta_N$ represent the change of chemical shift in the proton and nitrogen dimensions, respectively.

ITC. All samples were dissolved in 150 mM HEPES, pH 7.4, and the resultant solutions were degassed for 3 min prior to the loading into the ITC instrument. To investigate the binding affinity

of Cyt *c* to Aβ_{42}, the final concentrations of Cyt *c* (in the syringe) and Aβ_{42} (in the cell) were adjusted to 600 μM and 30 μM, respectively. Titration experiments composed of 25 injections were conducted. The injection volume was 2 μL for the first injection to minimize effects of bubbles and 10 μL for the remaining injections. To prevent Aβ_{42} aggregation, the temperature and stirring speed were set to 10 ^{o}C and 260 rpm, respectively. The initial delay was 1,800 s and the reference power was 10 μcal/s. The ITC thermogram was displayed after subtracting the dilution heat.

MD Simulation. All models of Cyt *c* and Aβ_{42} were simulated with the Amber16[15] software package. We selected a X-ray crystal structure of Cyt *c* (PDB 1HRC[16]). In the case of Aβ_{42}, its monomeric structure (Fig. 2a), which occupied the largest population (*ca*. 11%) in the ensembles, was chosen from our algorithm which uses multiple linear regression and NMR data of the structural ensembles of its monomers in the solution.[17] The Amber FF99SB force field[18] was used for both proteins and especially the Generalized Amber Force Field (GAFF)[19] was used to parameterize the covalent bonding parameters of the heme structure of Cyt *c* and atomic partial charges were computed as well. The Gaussian09 software[20] was utilized to achieve ESP potentials of the heme at HF/6-31G(d) level of theory. Moreover, the atomic partial charges were retrieved based on the Merz-Singh-Kollman algorithm. The initial distance between the Cyt *c* and Aβ_{42} was at least 6 Å. Total 88 replicas of randomly placed Aβ_{42} nearby the Cyt *c* were simulated. Simulation systems were immersed in octahedral solvation boxes filled with TIP3P[21] water molecules with a margin of 12 Å from the solvation boundary. Sodium ions [Na(I)] were added for electrostatic neutrality of the system which consists of approximately 46,000 atoms in total. The integration time step was 4 fs for all MD simulations. The MD simulations were held through the following procedure: (i) The preliminary procedure involved energy minimization of the system for 4,000 cycles. (ii) The solvated system was equilibrated with the Berendsen thermostat at 300 K using the NVT ensemble for 10 ns. (iii) An isobaric ensemble (NPT) was used for 20 ns where the pressure was controlled to maintain 1 atm with a relatively weaker restraint force constant (0.1 kcal/mol/Å^2). (iv) 200 ns equilibrium step was performed by the Langevin thermostat and the Monte Carlo barostat to keep the temperature at 300 K and pressure at 1 atm, respectively. As another aspect, the particle mesh Ewald method[22] was utilized to treat the long-range electrostatic interactions and the SHAKE algorithm was employed to constrain the hydrogens. We analyzed the structure of the dimeric species after 100 ns production.

ABTS Assay. Peroxidase-like activity of Cyt *c* was evaluated by ABTS assay. ABTS (160 μM),

H_2O_2 (80 μM), and Cyt *c* (5, 10, 15, 20, and 25 μM) were mixed and agitated at 25 °C for 15, 30, and 45 min. The absorbance values of oxidized ABTS were recorded at 750 nm. The measurements were conducted in triplicate.

DLS. Cyt *c* was incubated with Zn(II) and H_2O_2 for 0, 1, 2, 4, 8, and 12 h at 37 °C with constant agitation in 150 mM HEPES, pH 7.4. The samples (20 μL) were transferred to a 384-well microplate (Corning, ME, USA). The DLS data were acquired from 20 separate scans with an acquisition time of 10 s at 25 °C. The Dynamics software (Version 7.9.1.4) from Wyatt Technology (CA, USA) was used for data processing.

Cell Viability Studies. The human neuroblastoma SH-SY5Y cell line was purchased from the American Type Culture Collection (ATCC, Manassas, VA, USA). The cell line was maintained in media containing 50% minimum essential medium (MEM) and 50% F12 (GIBCO, Grand Island, NY, USA), and supplemented with 10% fetal bovine serum (FBS, GIBCO), 100 U/mL penicillin-streptomycin (GIBCO). Cells were grown and maintained at 37 °C in a humidified atmosphere with 5% CO_2. The cells used for our studies did not indicate mycoplasma contamination. Cell viability upon treatment with samples was determined by the MTT assay. $A\beta_{42}$ (50 μM) was pre-incubated with $ZnCl_2$ (50 μM), Cyt *c* (50 μM), and H_2O_2 (400 μM) for 12 h at 37 °C with constant agitation. Cells were seeded in a 96 well plate (10,000 cells in 100 μL per well) and treated with the resultant samples. The final concentrations of $A\beta_{42}$, $ZnCl_2$, Cyt *c*, and H_2O_2 were 10 μM, 10 μM, 10 μM, and 80 μM, respectively. After 24 h incubation, MTT [5 mg/mL in PBS (pH 7.4, GIBCO); 25 μL] was added to each well and the plate was incubated for 4 h at 37 °C. Formazan produced by cells was solubilized using an acidic solution of *N*,*N*-dimethylformamide (DMF; pH 4.5, 50% v/v, aq) and sodium dodecyl sulfate (SDS; 20% w/v) overnight at room temperature in the dark. The absorbance was measured at 600 nm by a microplate reader. The viability of cells was calculated relative to that of the cells containing an equivalent amount of the buffer solution (150 mM HEPES, pH 7.4). Data are represented as mean ± s.e.m (standard error of the mean) of three independent experiments.

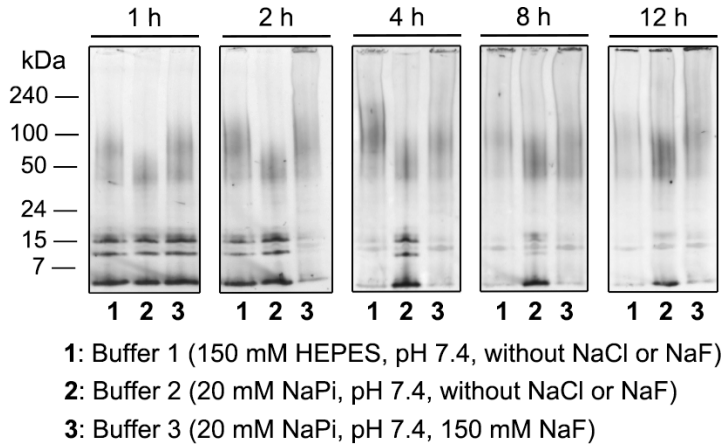

Fig. S1 Aggregation of $A\beta_{42}$ in three different buffered solutions. The size distribution of the resultant $A\beta_{42}$ species upon incubation with Cyt *c* for 1, 2, 4, 8, and 12 h in three different buffered solutions was analyzed by gel/Western blot using an anti-Aβ antibody (6E10). Conditions: [$A\beta_{42}$] = 25 μM; [Cyt *c*] = 25 μM; 37 °C; constant agitation (250 rpm).

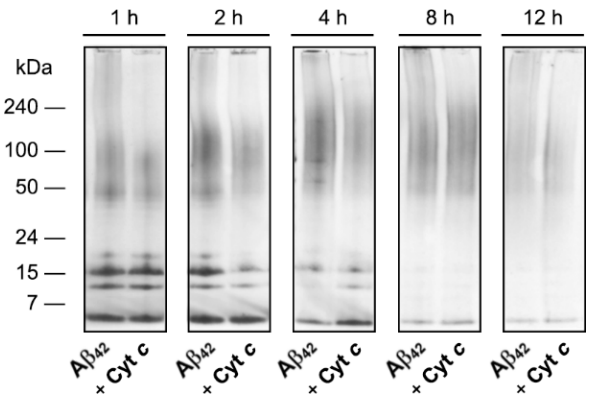

Fig. S2 Aggregation of $A\beta_{42}$ in an $A\beta_{42}$-to-Cyt *c* ratio of 10:1. The size distribution of the $A\beta_{42}$ species produced by incubation with Cyt *c* was analyzed by gel/Western blot using an anti-Aβ antibody (6E10). Conditions: [$A\beta_{42}$] = 25 μM; [Cyt *c*] = 2.5 μM; 20 mM NaPi buffer, pH 7.4, 150 mM NaF; 37 °C; constant agitation (250 rpm).

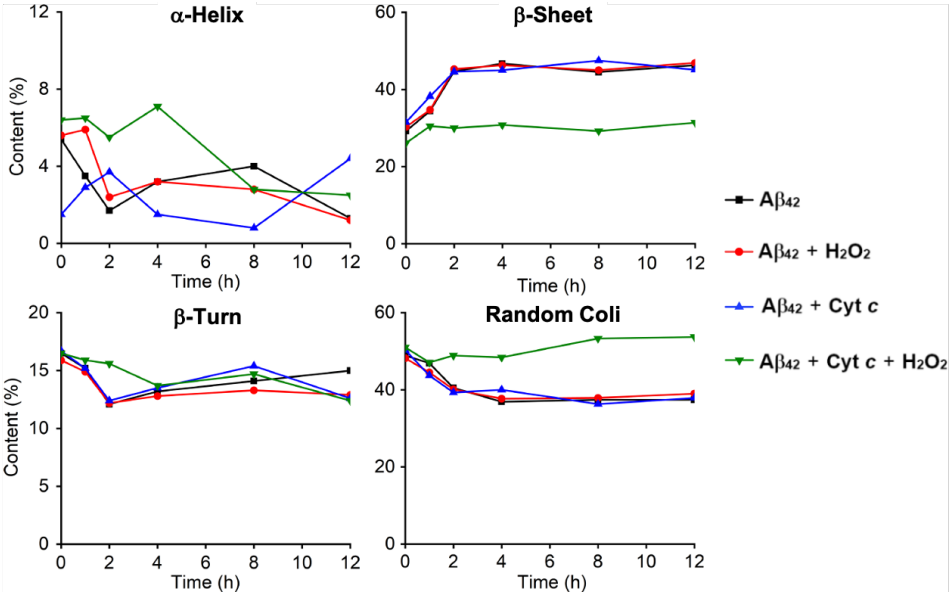

Fig. S3 Analysis of the contents of secondary structures of metal-free $A\beta_{42}$ upon aggregation in the absence and presence of either Cyt *c*, H_2O_2, or both. The corresponding CD spectra used for the analysis are shown in Fig. 1d.

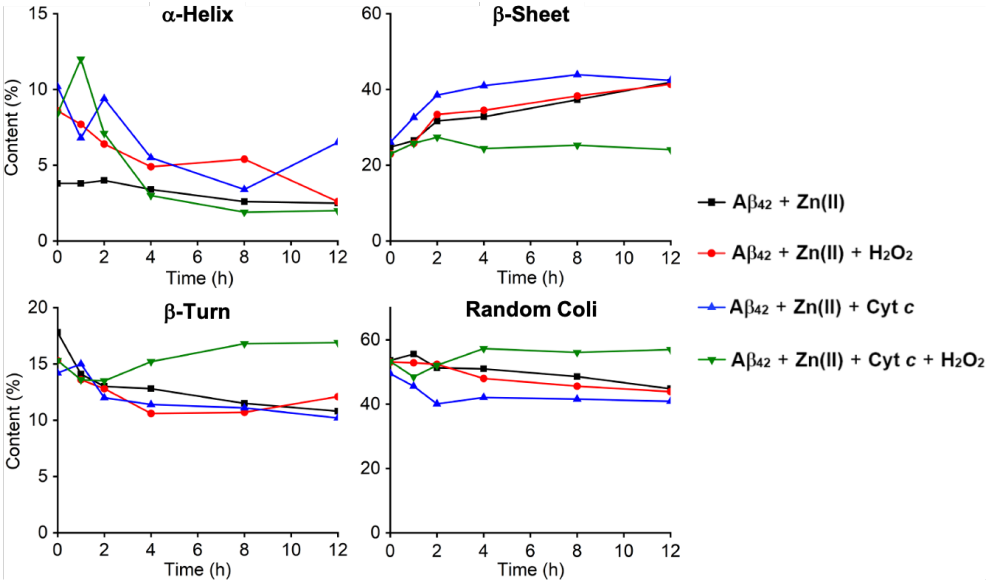

Fig. S4 Analysis of the contents of secondary structures of Zn(II)-treated Aβ_{42} upon aggregation in the absence and presence of either Cyt *c*, H_2O_2, or both. The corresponding CD spectra used for the analysis are shown in Fig. 1d.

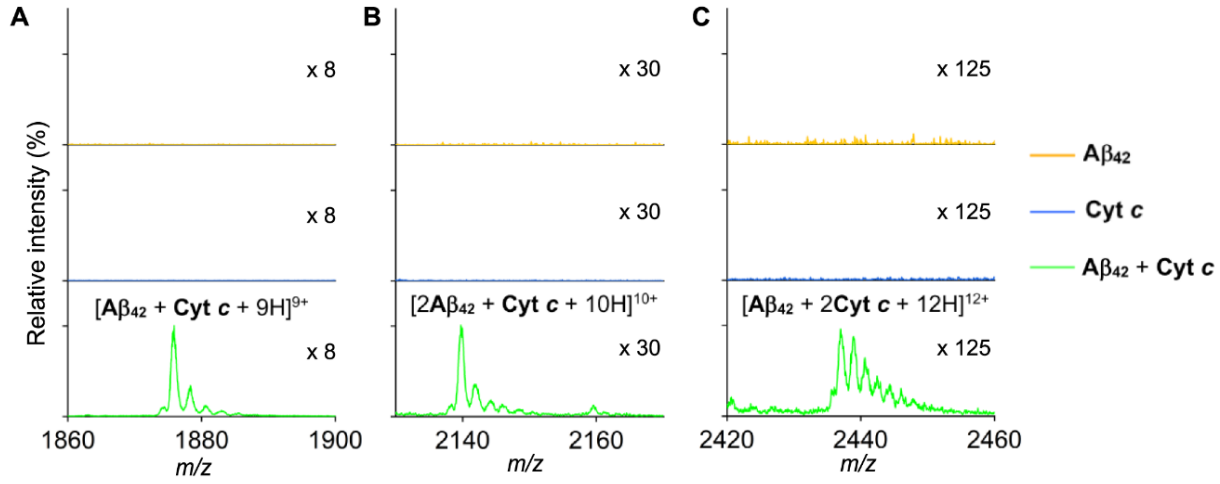

Fig. S5 ESI–MS spectra of Cyt *c*, Aβ_{42}, and the Cyt *c*–Aβ_{42} adducts. The adducts of Aβ_{42} and Cyt *c* in the Aβ_{42}-to-Cyt *c* ratios of (a) 1:1, (b) 2:1, and (c) 1:2 were found. Conditions: [Aβ_{42}] = 100 μM; [Cyt *c*] = 100 μM; 20 mM ammonium acetate, pH 7.4; 37 °C; 30 min incubation; no agitation. The 10-folded diluted samples were injected to the mass spectrometer.

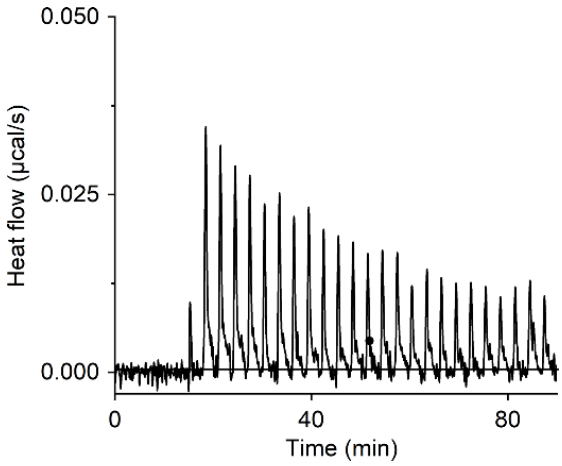

Fig. S6 ITC thermogram observed upon titrating Cyt *c* into Aβ_{42} after subtracting dilution heat. Conditions: [Aβ_{42}] = 30 μM (cell); [Cyt *c*] = 600 μM (syringe); 150 mM HEPES, pH 7.4.

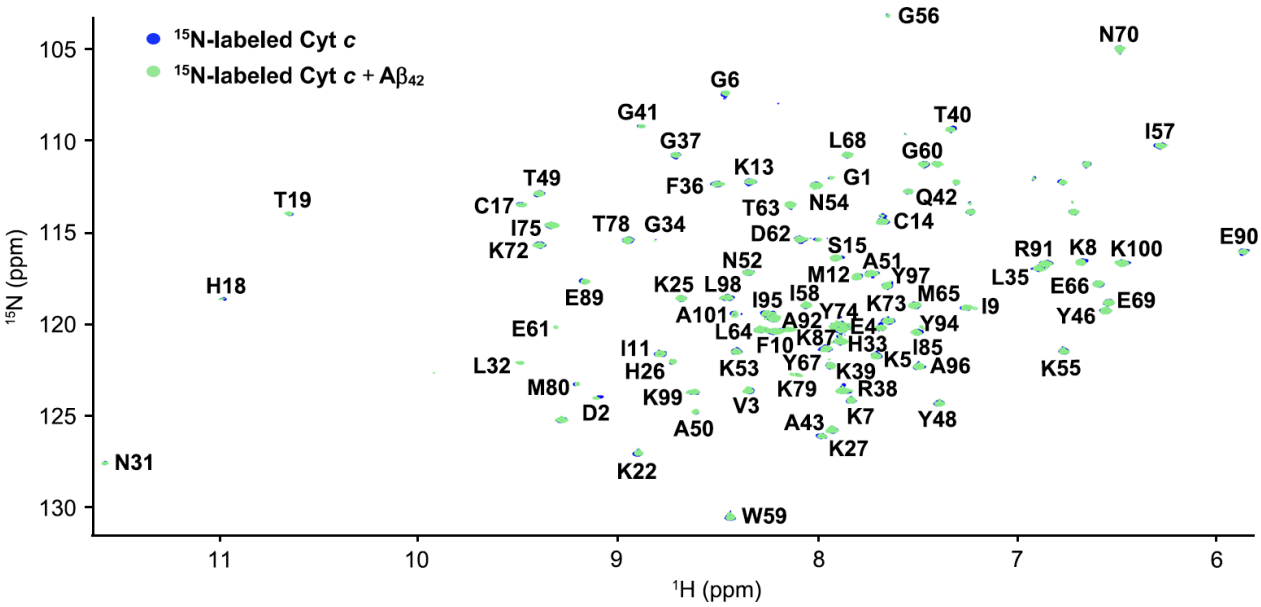

Fig. S7 2D ^{1}H–^{15}N HSQC NMR spectra of ^{15}N-labeled Cyt *c* with and without $A\beta_{42}$. The averaged CSPs and the change in the peak intensity are presented in Figure 2c. Conditions: [^{15}N-labeled Cyt *c*] = 20 μM; [$A\beta_{42}$] = 100 μM; 20 mM HEPES, pH 7.4; 10% v/v D_2O; 10 °C.

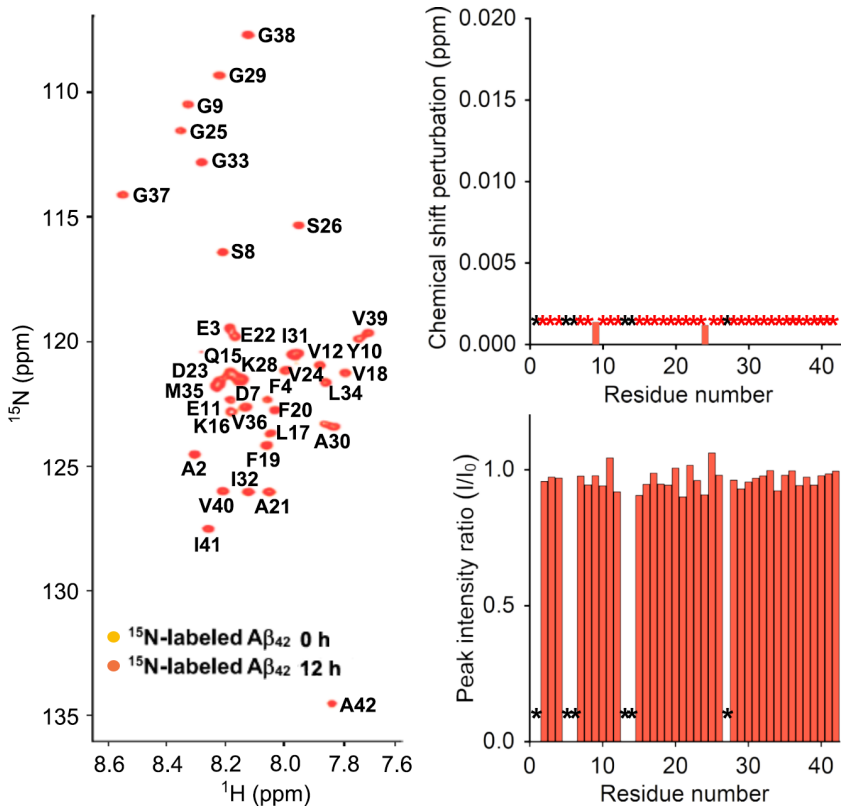

Fig. S8 2D ^{1}H–^{15}N SOFAST-HMQC NMR spectra of ^{15}N-labeled $A\beta_{42}$ incubated for 0 and 12 h. Black asterisks represent the amino acid residues not used for the analysis due to the overlapped peak position, and red asterisks indicate the amino acid residues without detectable CSPs. Conditions: [$A\beta_{42}$] = 40 μM; 20 mM HEPES, pH 7.4; 10% v/v D_2O; 10 °C.

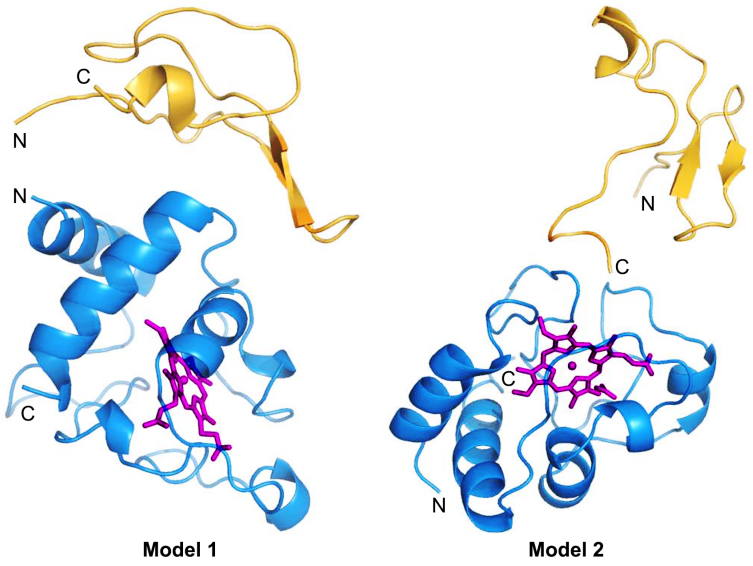

Fig. S9 Model 1 and 2 of the Cyt *c*–Aβ_{42} complexes.

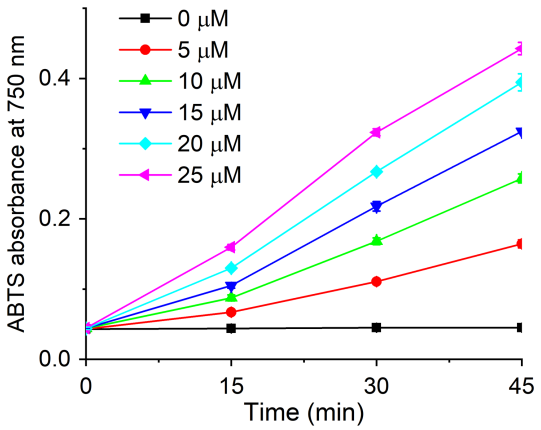

Fig. S10 Peroxidase-like activity of Cyt *c* measured by the ABTS assay. Conditions: [ABTS] = 160 μM; [H_2O_2] = 80 μM; [Cyt *c*] = 5, 10, 15, 20, and 25 μM; 25 °C; constant agitation (250 rpm).

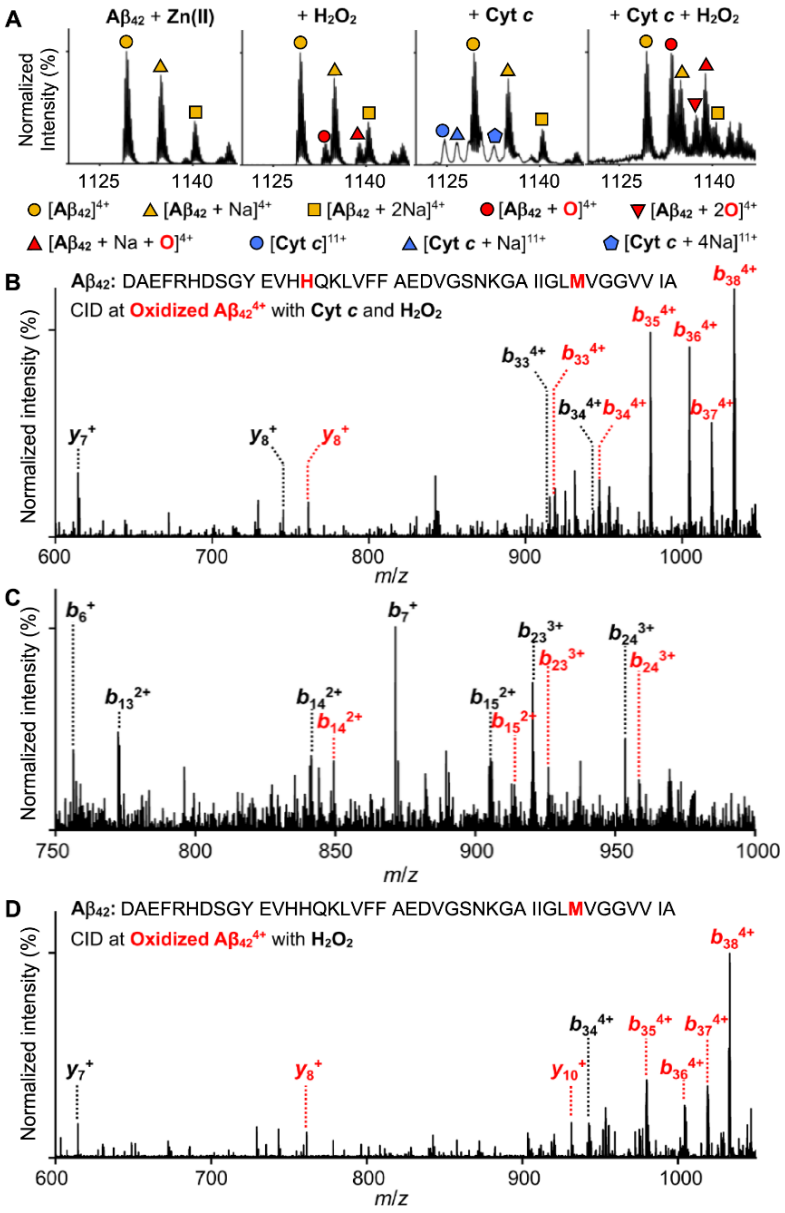

Fig. S11 Oxidation of $A\beta_{42}$ with Cyt *c* and H_2O_2 in the presence of Zn(II) detected by ESI–MS and ESI–MS^2. (a) ESI–MS spectra of +4-charged $A\beta_{42}$ incubated with Zn(II), Cyt *c*, and H_2O_2. Oxidized $A\beta_{42}^{4+}$ by Cyt *c* and H_2O_2 in the presence of Zn(II) [(b)1,133 *m*/*z* (oxidized $A\beta_{42}^{4+}$); (c) 1,139 *m*/*z* (an adduct of oxidized $A\beta_{42}^{4+}$ with Na^+)] were analyzed by ESI–MS^2. (d) ESI–MS^2 spectrum of oxidized $A\beta_{42}^{4+}$ produced by H_2O_2 in the presence of Zn(II). Conditions: [$A\beta_{42}$] = 100 μM; [Zn(II)] = 100 μM; [Cyt *c*] = 100 μM; [H_2O_2] = 1.6 mM; 20 mM ammonium acetate, pH 7.4; 37 °C; incubation for 30 min; no agitation. The 10-fold diluted samples were injected to the mass spectrometer.

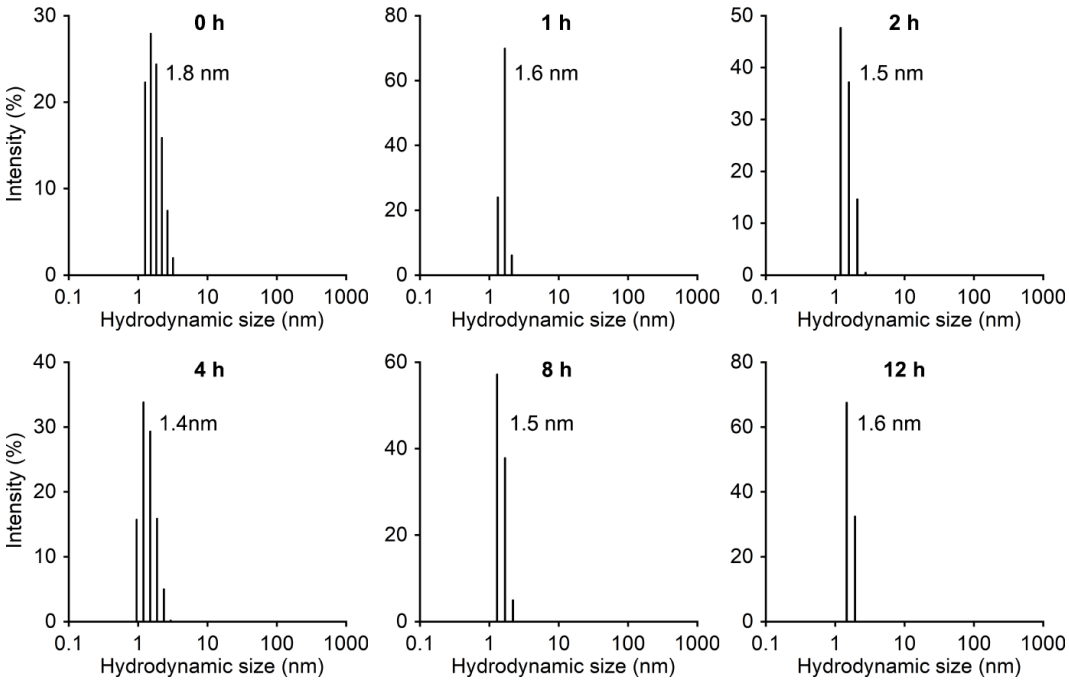

Fig. S12 Analysis of the R_H values of Cyt *c* upon incubation for 0, 1, 2, 4, 8, and 12 h by DLS. Conditions: [Cyt *c*] = 25 μM; 150 mM HEPES, pH 7.4; 37 °C; constant agitation (250 rpm).

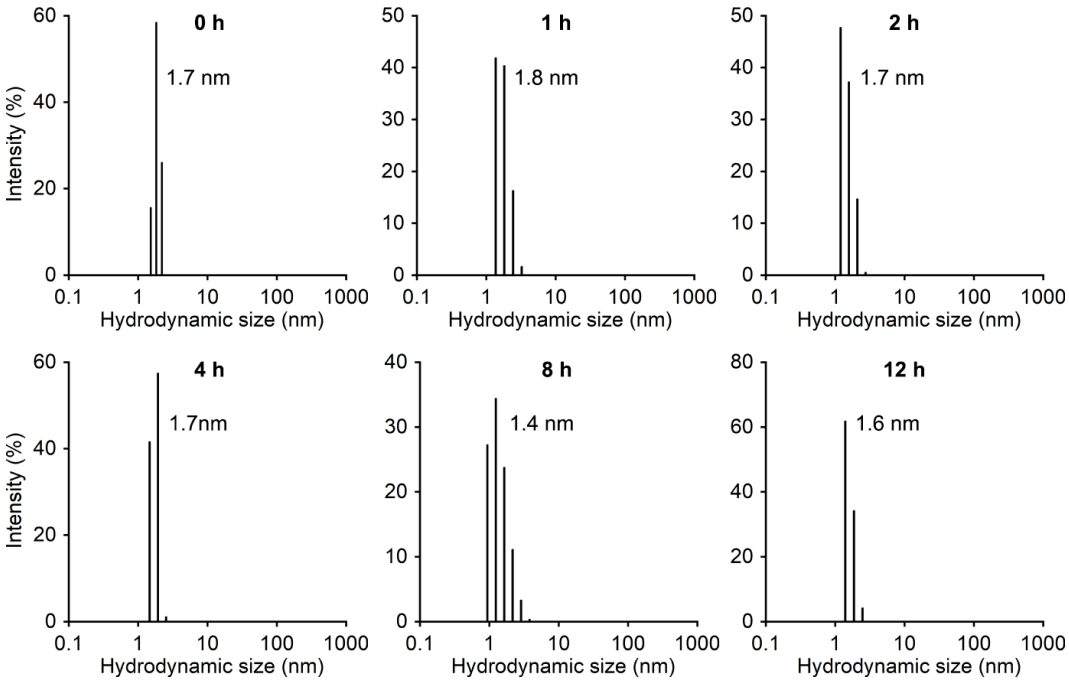

Fig. S13 Measurement of the the R_H values of Cyt *c* upon incubation with Zn(II) for 0, 1, 2, 4, 8, and 12 h by DLS. Conditions: [Cyt *c*] = 25 μM; [Zn(II)] = 25 μM; 150 mM HEPES, pH 7.4; 37 °C; constant agitation (250 rpm).

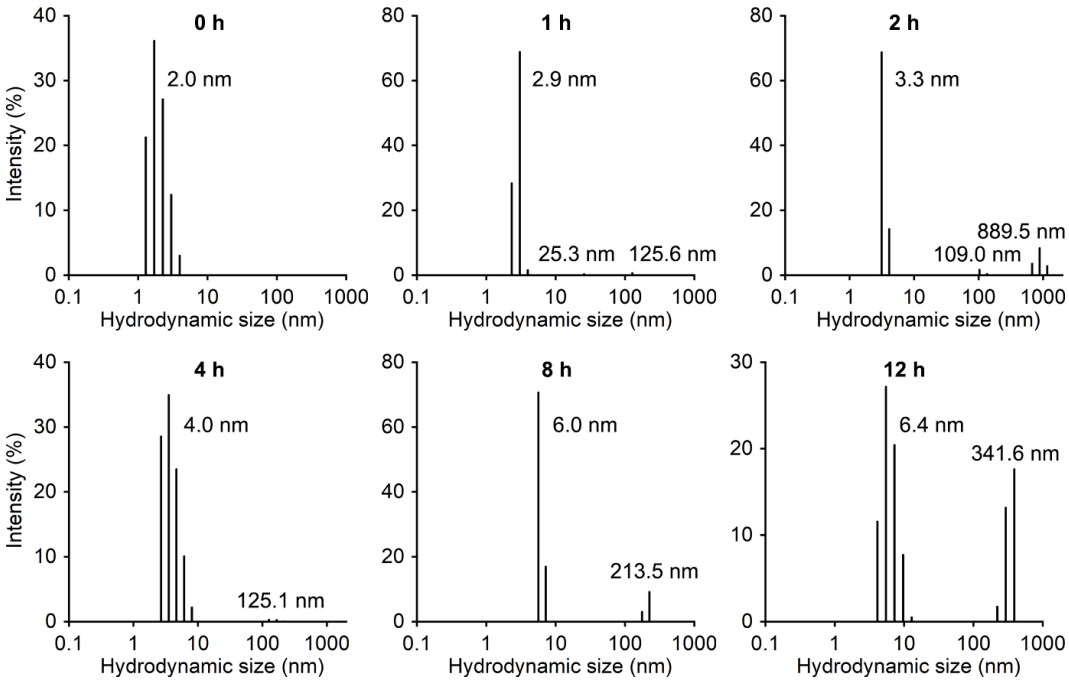

Fig. S14 Change in the the R_H values of Cyt *c* upon incubation with H_2O_2 for 0, 1, 2, 4, 8, and 12 h monitored by DLS. Conditions: [Cyt *c*] = 25 μM; [H_2O_2] = 200 μM; 150 mM HEPES, pH 7.4; 37 °C; constant agitation (250 rpm).

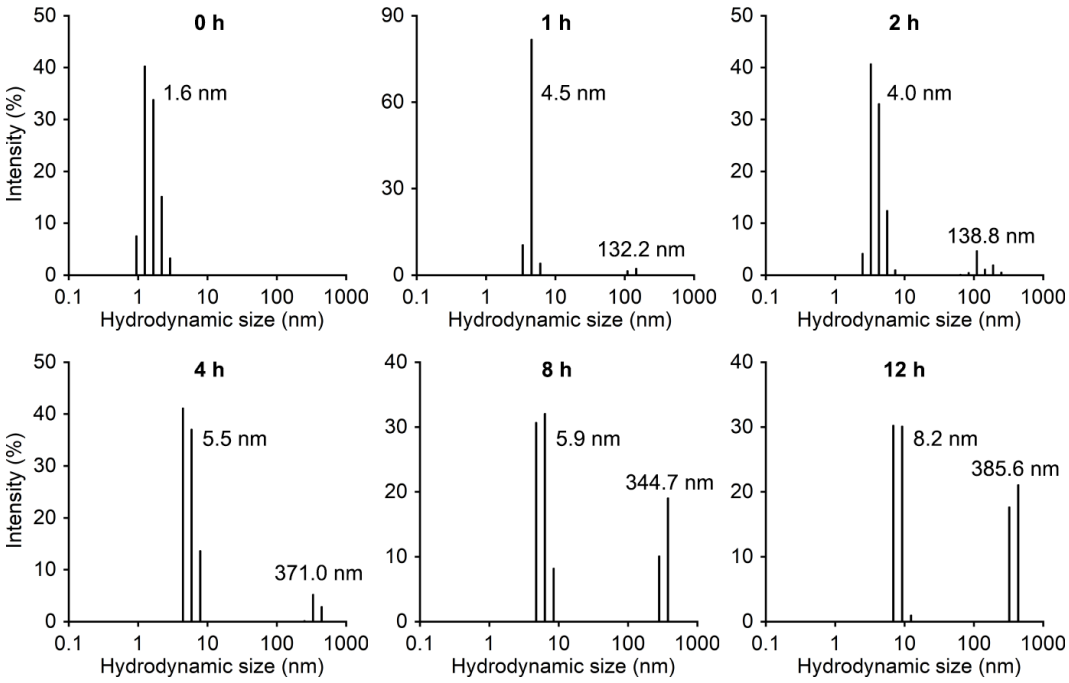

Fig. S15 Analysis of the the R_H values of Cyt *c* upon incubation with Zn(II) and H_2O_2 for 0, 1, 2, 4, 8, and 12 h by DLS. Conditions: [Cyt *c*] = 25 μM; [Zn(II)] = 25 μM; [H_2O_2] = 200 μM; 150 mM HEPES, pH 7.4; 37 °C; constant agitation (250 rpm).

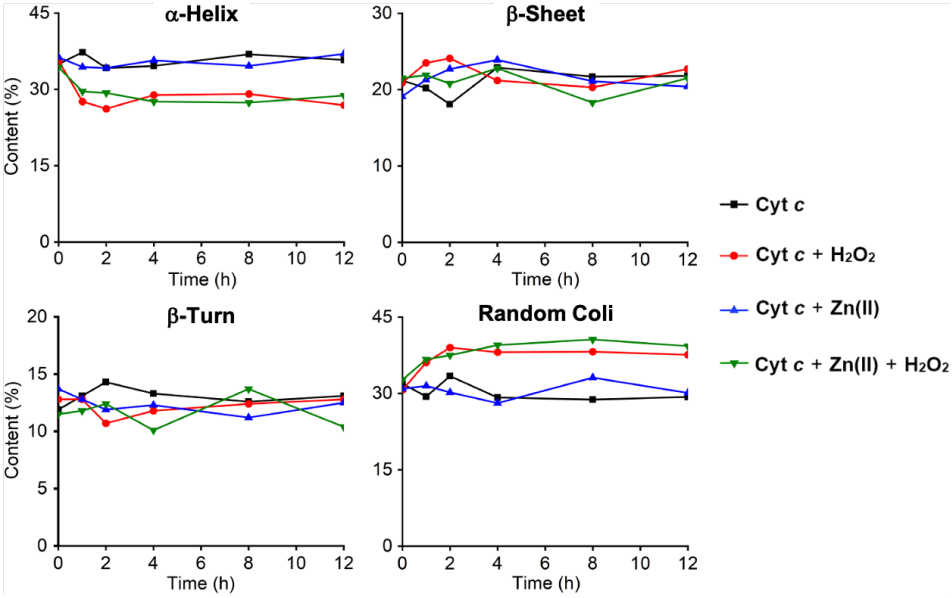

Fig. S16 Analysis of the contents of the secondary structures of Cyt *c* upon aggregation in the presence of either Zn(II), H_2O_2, or both. The corresponding CD spectra used for the analysis are presented in Fig. 4d.

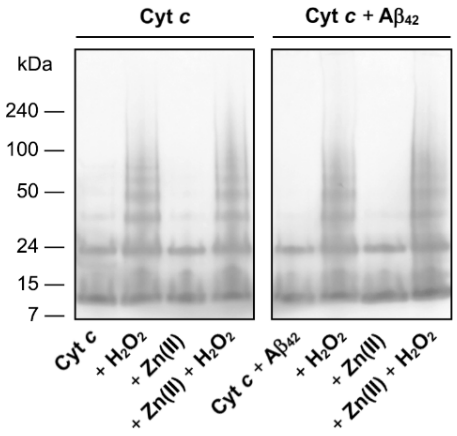

Fig. S17 Impact of $A\beta_{42}$ on the aggregation of Cyt *c*. The size distribution of the resultant Cyt *c* species upon incubation with $A\beta_{42}$, Zn(II), and H_2O_2 for 12 h was analyzed by gel/Western blot using an anti-Cyt *c* antibody. Conditions: [Cyt *c*] = 25 μM; [$A\beta_{42}$] = 25 μM; [Zn(II)] = 25 μM; [H_2O_2] = 200 μM; 150 mM HEPES buffer, pH 7.4; 37 °C; constant agitation (250 rpm).

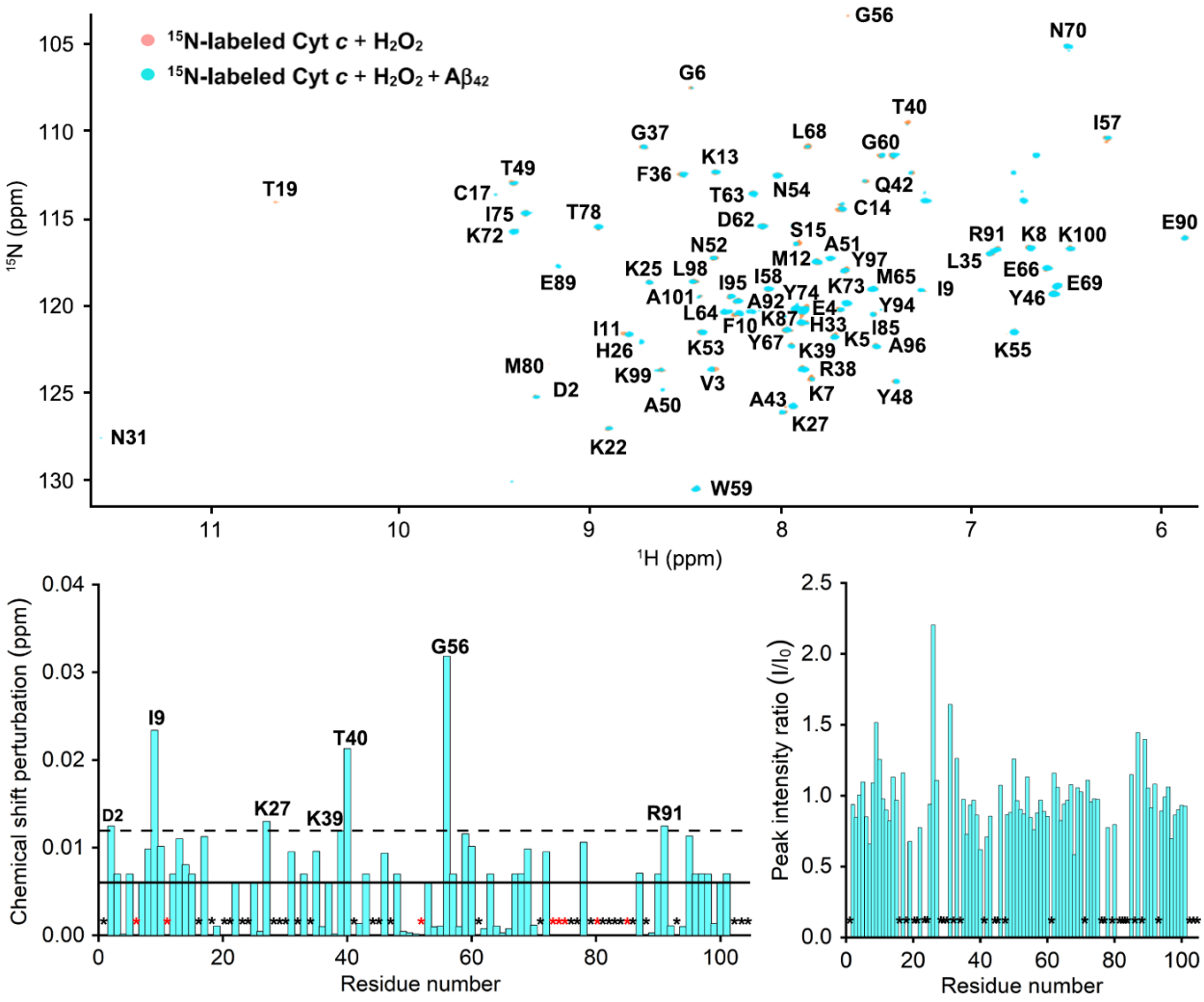

Fig. S18 2D ^{1}H–^{15}N HSQC NMR spectra of ^{15}N-labeled Cyt *c* with H_2O_2 in the absence and presence of $A\beta_{42}$. The average of CSPs and the average plus one standard deviation are depicted with solid and dashed lines, respectively. Black asterisks represent the amino acid residues that cannot be resolved for analysis, and red asterisks indicate the amino acid residues without detectable CSPs. Conditions: [^{15}N-labeled Cyt *c*] = 20 μM; [H_2O_2] = 160 μM; [$A\beta_{42}$] = 100 μM; 20 mM HEPES, pH 7.4; 10% v/v D_2O; 10 °C.

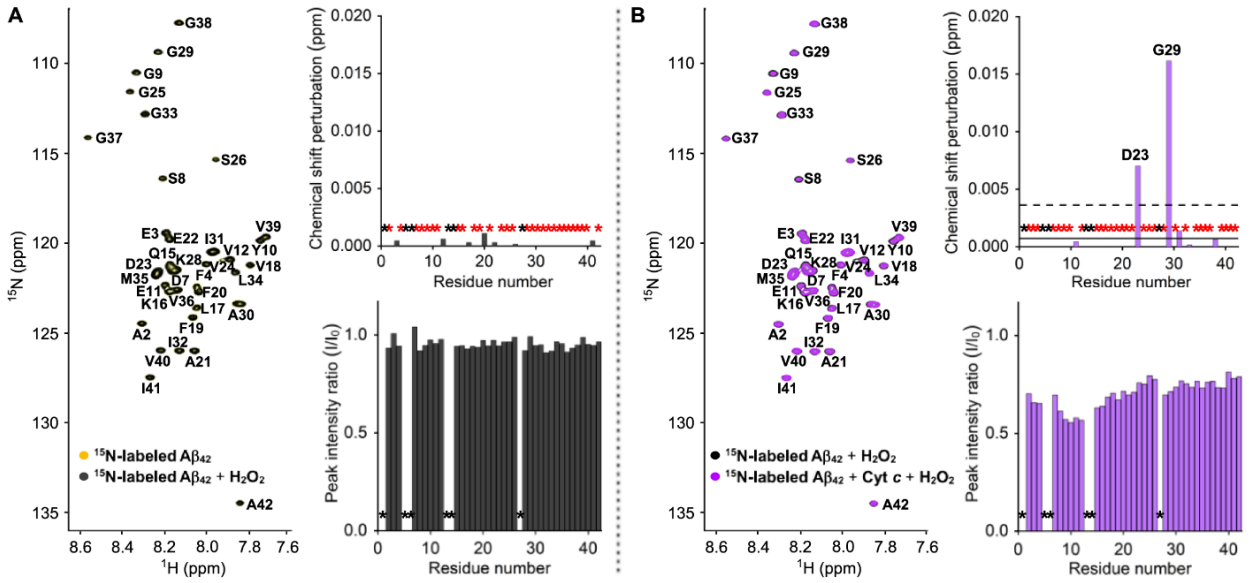

Fig. S19 2D ^{1}H–^{15}N SOFAST–HMQC NMR spectra of ^{15}N-labeled Aβ$_{42}$ in the presence of either Cyt *c*, H_2O_2, or both. (a) 2D ^{1}H–^{15}N SOFAST–HMQC NMR spectra (800 MHz) of ^{15}N-labeled Aβ$_{42}$ monomer with and without H_2O_2. The average of CSPs and the average plus one standard deviation are depicted with solid and dashed lines, respectively. Black asterisks represent the amino acid residues that cannot be resolved for analysis, and red asterisks indicate the amino acid residues without detectable CSPs. (b) 2D ^{1}H–^{15}N SOFAST–HMQC NMR spectra of ^{15}N-labeled Aβ$_{42}$ monomer with H_2O_2 in the absence and presence of Cyt *c*. Conditions: [^{15}N-labeled Aβ$_{42}$] = 40 μM; [H_2O_2] = 1.6 mM; [Cyt *c*] = 200 μM; 150 mM HEPES, pH 7.4; 10% v/v D_2O; 10 °C.

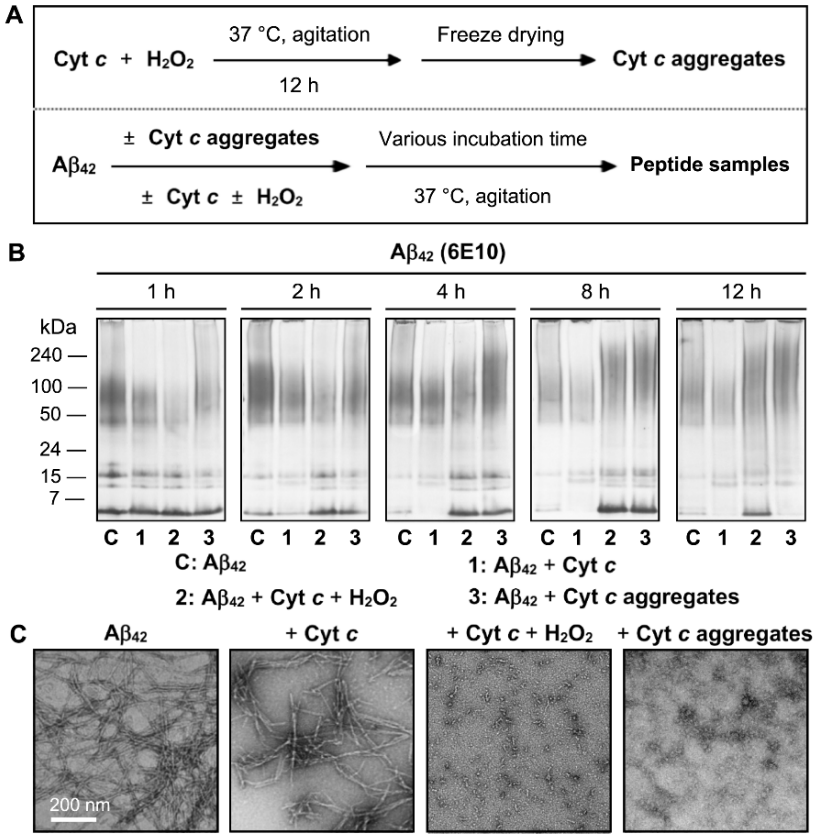

Fig. S20 Influence of amorphous Cyt *c* aggregates on $A\beta_{42}$ aggregation. (a) Scheme of $A\beta_{42}$ aggregation experiments with and without amorphous Cyt *c* aggregates. Amorphous Cyt *c* aggregates were prepared by incubating Cyt *c* with H_2O_2 for 12 h and the solution was removed by lyophilization. Then resultant amorphous Cyt *c* aggregates were redissolved and added into the solution of $A\beta_{42}$. (b) The size distribution of the resultant $A\beta_{42}$ species analyzed by gel/Western blot using an anti-Aβ antibody (6E10). (c) Morphology of the peptide aggregates produced after 12 h incubation visualized by TEM. Conditions: [$A\beta_{42}$] = 25 μM; [Cyt *c*] = 25 μM; [H_2O_2] = 200 μM; 150 mM HEPES buffer, pH 7.4; 37 °C; constant agitation (250 rpm).

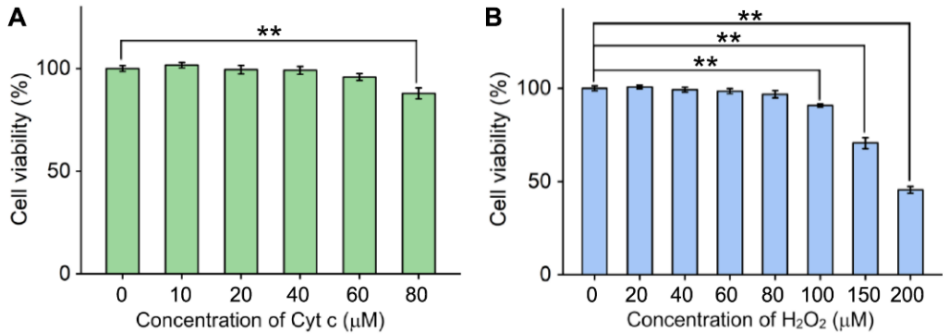

Fig. S21 Cytotoxicity of Cyt *c* and H_2O_2. SH–SY5Y cells were treated with (a) Cyt *c* or (b) H_2O_2 followed by 24 h incubation. Cell viability, determined by the MTT assay, was calculated in comparison to that with an equivalent amount of the buffered solution. Conditions: [Cyt *c*] = 10, 20, 40, 60, and 80 μM; [H_2O_2] = 20, 40, 60, 80, 100, 150, and 200 μM. Data are represented as mean ± s.e.m. ***P* < 0.01 by Student's *t*-test.

References

1. T. Ikenoue, Y. H. Lee, J. Kardos, M. Saiki, H. Yagi, Y. Kawata and Y. Goto, *Angew. Chem. Int. Ed.*, 2014, **53**, 7799-7804.
2. D. S. Doering and P. Matsudaira, *Biochemistry*, 1996, **35**, 12677-12685.
3. E. Nam, J. Han, S. Choi and M. H. Lim, *Chem. Commun.*, 2021, **57**, 7637-7640.
4. J. Han, H. J. Lee, K. Y. Kim, G. Nam, J. Chae and M. H. Lim, *Proc. Natl. Acad. Sci. U. S. A.*, 2020, **117**, 5160-5167.
5. E. Margoliash and N. Frohwirt, *Biochem. J.*, 1959, **71**, 570-572.
6. M. J. Abraham-Juárez, *BioProtoc.*, 2019, **9**, e3257.
7 A. Micsonai, F. Wien, L. Kernya, Y. H. Lee, Y. Goto, M. Refregiers and J. Kardos, *Proc. Natl. Acad. Sci. U. S. A.*, 2015, **112**, E3095-3103.
8. M. Kim, J. Kang, M. Lee, J. Han, G. Nam, E. Tak, M. S. Kim, H. J. Lee, E. Nam, J. Park, S. J. Oh, J. Y. Lee, J. Y. Lee, M. H. Baik and M. H. Lim, *J. Am. Chem. Soc.*, 2020, **142**, 8183-8193.
9. K. Sakamoto, M. Kamiya, M. Imai, K. Shinzawa-Itoh, T. Uchida, K. Kawano, S. Yoshikawa and K. Ishimori, *Proc. Natl. Acad. Sci. U. S. A.*, 2011, **108**, 12271-12276.
10. F. Delaglio, S. Grzesiek, G. W. Vuister, G. Zhu, J. Pfeifer and A. Bax, *J. Biomol. NMR*, 1995, **6**, 277-293.
11. Sparky 3, https://www.cgl.ucsf.edu/home/sparky/, (accessed July 2021).
12. Y. Yan and C. Wang, *J. Mol. Biol.*, 2006, **364**, 853-862.
13. K. Sakamoto, M. Kamiya, T. Uchida, K. Kawano and K. Ishimori, *Biochem. Biophys. Res. Commun.*, 2010, **398**, 231-236.
14. F. A. Mulder, D. Schipper, R. Bott and R. Boelens, *J. Mol. Biol.*, 1999, **292**, 111-123.
15. D. Case, R. Betz, D. S. Cerutti, T. Cheatham, T. Darden, R. Duke, T. J. Giese, H. Gohlke, A. Götz, N. Homeyer, S. Izadi, P. Janowski, J. Kaus, A. Kovalenko, T.-S. Lee, S. LeGrand, P. Li, C. Lin, T. Luchko and P. Kollman, *Amber 16, University of California, San Francisco*, 2016.
16. G. W. Bushnell, G. V. Louie and G. D. Brayer, *J. Mol. Biol.*, 1990, **214**, 585-595.
17. W. Yang, B. S. Kim, Y. Lin, D. Ito, J. H. Kim, Y.-H. Lee and W. Yu, *bioRxiv*, 2021, 2021.2008.2023.457317.
18. V. Hornak, R. Abel, A. Okur, B. Strockbine, A. Roitberg and C. Simmerling, *Proteins*, 2006, **65**, 712-725.
19. J. Wang, R. M. Wolf, J. W. Caldwell, P. A. Kollman and D. A. Case, *J. Comput. Chem.*, 2004, **25**, 1157-1174.
20. M. J. Frisch, G. W. Trucks, H. B. Schlegel, G. E. Scuseria, M. A. Robb, J. R. Cheeseman, G. Scalmani, V. Barone, B. Mennucci and G. A. Petersson, *Wallingford, CT*, 2009, **32**, 5648-5652.

21. W. L. Jorgensen, J. Chandrasekhar, J. D. Madura, R. W. Impey and M. L. Klein, *J. Chem. Phys.*, 1983, **79**, 926-935.
22. T. Darden, D. York and L. Pedersen, *J. Chem. Phys.*, 1993, **98**, 10089-10092.